Cation radical salts of cyano(ethylenedithio)tetrathiafulvalene with halogenated anions: annihilation of the CN···Hal interaction and stabilisation of conducting, antiferromagnetic square or chain-type salts†

Thomas Devic,[a] Josep N. Bertran,[a] Benoît Domercq,[a] Enric Canadell,[b] Narcis Avarvari,[a] Pascale Auban-Senzier[c] and Marc Fourmigué*[a]

[a] *Sciences Moléculaires aux Interfaces (CNRS FRE 2068), Institut des Matériaux Jean Rouxel, BP32229, 2, rue de la Houssinière, 44322 Nantes cedex 3, France. E-mail: fourmigue@cnrs-imn.fr*

[b] *Institut de Ciència de Materials de Barcelona (CSIC), Campus de la UAB, 08193 Bellaterra, Spain*

[c] *Laboratoire de Physique des Solides (CNRS UMR 8502), Université Paris-Sud, Bât. 510, 91405 Orsay cedex, France*

Received (in Strasbourg, France) 25th May 2001, Accepted 7th August 2001
First published as an Advance Article on the web 22nd October 2001

The synthesis, X-ray crystal structure and electrochemical properties of 3-cyano-3′,4′-ethylenedithiotetrathiafulvalene (EDT-TTF-CN, **1**) are described together with electrocrystallisation experiments in the presence of various halogenated anions, I_3^-, $FeBr_4^-$, $InBr_4^-$, $AuBr_4^-$, $Mo_6Br_{14}^{2-}$, $Mo_6Cl_8Br_6^{2-}$. X-Ray crystal structures are described for each salt, characterised by a systematic absence of any short and directional CN···Hal interactions, convincing evidence of the electrostatic character of this interaction, which is enhanced in the opposite situation where cationic halogenated tetrathiafulvalenes are associated with cyanide anions such as $Ag(CN)_2^-$. This behaviour is further rationalised by atomic population calculations on TTF-CN and [TTF-CN]$^{\cdot+}$, which confirm the strong decrease of the negatively charged character of the nitrogen atom upon TTF-CN oxidation to [TTF-CN]$^{\cdot+}$. A conducting mixed-valence salt is obtained in $[\mathbf{1}]_2[I_3]$, which exhibits an unusual structure with the I_3^- anions embedded in the organic conducting layer. All the other salts contain fully oxidised $[\mathbf{1}]^{\cdot+}$ radical cations, associated into diamagnetic diads in $[\mathbf{1}][I_3]$, $[\mathbf{1}]_2[Mo_6Br_{14}][CH_3CN]_4$ and $[\mathbf{1}]_2[Mo_6Cl_8Br_6][CH_3CN]_4$, into spin chains in the two isostructural $[\mathbf{1}][FeBr_4]$ and $[\mathbf{1}][InBr_4]$ salts and into a quadratic two-dimensional spin system in $[\mathbf{1}][AuBr_4]$.

In the numerous molecular conductors derived from tetrathiafulvalene donor molecules that have been investigated up to date,[1] the introduction of specific substituents on the TTF core,[2] which are able to engage in weak intermolecular interactions such as *hydrogen bonding*, is particularly appealing. Several conducting salts have already been described that involve a variety of functionalities such as alcohols [EDT-TTF-CH_2OH,[3] $TTF(CH_2OH)_4$],[4] amides (EDT-TTF-CONHR)[5] or thioamides (TTF-CSNHR).[6] More recently, halide-functionalised TTFs such as TTF-I,[7] EDT-TTF-I,[8] EDO-TTF-I_2[9] or DIETS[10] have also been described that engage in so-called *halogen bonding*,[11] that is Hal···Hal interactions with halogenated anions[12] or linear CN···Hal interactions[13,14] with cyano anions such as $Ag(CN)_2^-$, $Pd(CN)_4^{2-}$ or $[Pd(mnt)_2]^{2-}$.

Organic nitriles are also able to sustain intermolecular interactions in the solid state through the lone pair of the nitrogen atom, either by hydrogen bonding with hydrogen bond donors,[15] by halogen bonding with organic halides[16,17] or by metal co-ordination. In this respect, tetrathiafulvalenes bearing one,[18] two[19,20] or four CN groups[21] have already been synthesised but none of them ever engaged in cation radical salts. This failure most probably stems from the strong electron-withdrawing effect of the nitrile substituent, leading to a poor electron-donor character. For example, $TTF(CN)_4$ oxidises[21] at 1.12 and 1.22 V *vs.* SCE (TTF: 0.33 and 0.71 V *vs.* SCE). We can, however, expect that placing only one CN group on the ethylenedithiotetrathiafulvalene molecule (EDT-TTF) will afford a reasonably good donor molecule, which would combine the effect of the SCH_2CH_2S substitution for the formation of two-dimensional, layered salts, with the potentialities offered by the CN group through hydrogen or halogen bonding. In this paper, we describe the synthesis of 3-cyano-3′,4′-ethylenedithiotetrathiafulvalene (**1**), analyse its electrochemical properties and the structures of a variety of cation radical salts of **1** with highly halogenated anions of different shapes and charges, be they linear (I_3^-), tetrahedral ($FeBr_4^-$, $InBr_4^-$), square planar ($AuBr_4^-$) or complex clusters ($Mo_6Br_{14}^{2-}$, $Mo_6Cl_8Br_6^{2-}$).

Results

The novel donor molecule **1** has been prepared by coupling[19,21] 4-cyano-1,3-dithiole-2-one (**3**), obtained from the trithiocarbonate **2**,[22] with **4** in neat $P(OMe)_3$. **1** was obtained in 36% yield after chromatographic separation from the symmetrical coupling product (*Z*,*E*)-$(CN)_2$TTF (Scheme 1). Note that the latter was not available from the dilithiation of TTF, which affords *o*-$(CN)_2$TTF.[18] Compound **1** crystallises in the triclinic system, space group $P\bar{1}$, with one molecule in a

† Electronic supplementary information (ESI) available: conditions of the electrocrystallisation experiment. See http://www.rsc.org/suppdata/nj/b1/b104640n/

 DOI: 10.1039/b104640n

Table 1 Degree of charge transfer (ρ), IR CN stretching frequencies (cm^{-1}) and important bond distances in **1** (in Å) in its different oxidation states. See Fig. 1 for the definition of a, b, b′, c, c′, d, d′. Note that the distinctions between b and b′, c and c′ do not hold in the two I_3^- salts and the salts with $Mo_6Br_{14}^{2-}$ and $Mo_6Cl_8Br_6^{2-}$ in which the cyano group is disordered over two positions

Compound	ρ	ν_{CN}	a	b, b′	c, c′	d, d′
Neutral **1**	0	2214	1.348(8)	1.852(6), 1.811(7)	1.816(7), 1.843(6)	1.760(7), 1.751(6)
$[\mathbf{1}]_2[I_3]$: mol A	0.5	2224	1.377(9)	1.733(7), 1.741(7)	1.734(7), 1.734(7)	Disordered CN
mol B			1.368(9)	1.734(7), 1.745(7)	1.733(7), 1.734(7)	Disordered CN
$[\mathbf{1}][I_3]$	1	2234	1.384(7)	1.728(5), 1.726(5)	1.735(5), 1.717(5)	Disordered CN
$[\mathbf{1}][FeBr_4]$	1	2232	1.358(9)	1.717(7), 1.724(7)	1.722(7), 1.736(7)	1.732(7), 1.722(7)
$[\mathbf{1}][InBr_4]$	1	2230.6	1.390(6)	1.723(5), 1.728(5)	1.715(5), 1.713(5)	1.748(5), 1.711(5)
$[\mathbf{1}][AuBr_4]$	1	2235.5	1.390(15)	1.711(11), 1.726(11)	1.720(12), 1.711(11)	1.73(1), 1.71(1)
$[\mathbf{1}]_2[Mo_6Cl_8Br_6][CH_3CN]_4$	1	2230.5	1.38(2)	1.736(18), 1.712(13)	1.721(13), 1.723(15)	Disordered CN
$[\mathbf{1}]_2[Mo_6Br_{14}][CH_3CN]_4$	1	2230.1	1.382(8)	1.732(6), 1.732(5)	1.707(6), 1.722(5)	Disordered CN

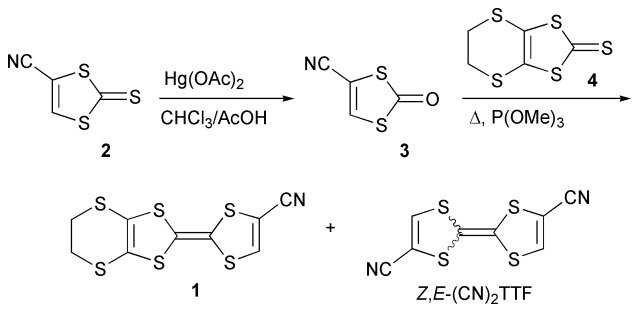

Scheme 1

general position in the unit cell (Fig. 1) having an essentially planar conformation.[23] Bond length distortions (particularly d > d′) within the dithiole ring bearing the CN group (Table 1) reflect the polarisation imposed by the electron-withdrawing group, as already observed on the TTF core with ester,[24] amide[25] or thioamide[6] substituents. The absence of any short C–H···N distance suggests that H-bonding is not involved in the packing of **1**. The donor molecule oxidises reversibly at 0.65 and 1.0 V *vs.* SCE in PhCN, illustrating the sizeable but limited electron-withdrawing effect of the cyano group since EDT-TTF itself oxidises at 0.43 and 0.83 V *vs.* SCE under the same conditions. This increase of the first oxidation potential is twice as large in (*Z*,*E*)-dicyanotetrathiafulvalene, which oxidises at 0.86 and 1.15 V *vs.* SCE, when compared with TTF itself which oxidises at 0.40 and 0.86 V *vs.* SCE in PhCN.[26] The electrocrystallisation of **1** was performed with several iodo and bromo complex anions in order to favour the possible setting of CN···Hal interactions in the solid state. Two different I_3^- salts, of 1 : 1 and 2 : 1 stoichiometry, were obtained in the presence of $[n\text{-}Bu_4N][I_3]$ in the same electrocrystallisation experiments in variable proportions, depending on the solvent used. The electrocrystallisation of **1** in the presence of $FeBr_4^-$ (as the $n\text{-}Et_4N^+$ salt) and the isosteric diamagnetic $InBr_4^-$ analogue afforded two isostructural salts of 1 : 1 stoichiometry. Another 1 : 1 salt was obtained with the square-planar $AuBr_4^-$ anion while the electrocrystallisation in the presence of the octahedral molybdenum cluster anions $Mo_6Cl_8Br_6^{2-}$ and $Mo_6Br_{14}^{2-}$ afforded two isostructural salts of 2 : 1 stoichiometry.

The 1 : 1 salt with I_3^- crystallises in the triclinic system, space group $P\bar{1}$ with one oxidised donor molecule and one

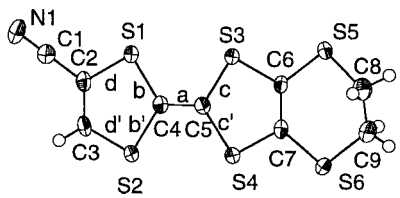

Fig. 1 ORTEP view of neutral **1**. Thermal ellipsoids are represented at the 50% probability level.

I_3^- anion in a general position in the unit cell [Fig. 2(a)]. The 2 : 1 salt crystallises in the triclinic system, space group $P\bar{1}$ with two crystallographically independent, partially oxidised molecules in general positions in the unit cell and two I_3^- anions, each of them on an inversion centre [Fig. 2(b)].[27] The intramolecular bond lengths follow the expected trends (Table 1) with a lengthening of the central C=C bond and shortening of the C–S bonds when increasing the oxidation state. Note also the increase in the IR ν(C≡N) stretching frequency upon oxidation, which is attributable to the antibonding character of the CN bond in the donor's HOMO (see below). In both 1 : 1 and 2 : 1 salts, the cyano group is disordered on the two carbon atoms of the TTF moiety with a 50 : 50 occupation ratio. The organic molecules are associated into inversion-centred overlap-stabilised diads with a short plane-to-plane distance, 3.365(1) Å in $[\mathbf{1}][I_3]$ and 3.436(2) Å in $[\mathbf{1}]_2[I_3]$, with the longer one associated, as expected, with the mixed-valence $[\mathbf{1}]_2^{\cdot+}$ moiety of the 2 : 1 salt. These diads alternate with the I_3^- anions within mixed organic–inorganic layers in both salts (Fig. 2). These layers are connected to each other through the organic donor molecules by C–H···N hydrogen bonds involving the hydrogen atom located *ortho* to the cyano group (Fig. 3), giving rise to a cyclic motif already identified in the crystal structure of 1,4-dicyanobenzene[28] and whose structural characteristics are collected in Table 2 for the 1 : 1 salt. Of particular note also is the complete absence of any short CN···I contacts. Indeed, as reported in Table 3, the shortest N···I distances are far above the sum of the van der Waals radii and the relative orientation of the CN and I_3^- moieties does not exhibit the linear arrangement ($\theta_1 \approx \theta_2 \approx 180°$) usually observed in CN···I interactions. From an electronic point of view, in the 1 : 1 salt, the formally unpaired electrons of the two radical cations are paired in the low-lying bonding combination of the two individual SOMOS, characterised by a strong $\beta_{HOMO\cdots HOMO}$ interaction energy,[29] calculated here to be 1.02 eV. We therefore expect an insulating, diamagnetic behaviour. Since both I_3^- salts were obtained simultaneously and could not be easily separated, SQUID susceptibility measurements were not performed but single crystal conductivity measurements performed on the mixed-valence, 2 : 1 salt show a high room temperature conductivity ($\sigma_{RT} = 0.5$ S cm^{-1}) and a semi-conducting behaviour upon cooling with an activation energy around 2000 K (Fig. 4). This high conductivity is all the more interesting given the very specific structure of this salt. Indeed, in molecular conductors based on EDT- or BEDT-TTF molecules, segregation between the cationic

Table 2 Hydrogen bond characteristics of the two disordered cyclic motifs in $[\mathbf{1}][I_3]$

	d[(C)H···N]/Å	d[C(H)···N]/Å	∠C–H···N/°
C1–H1···N1B	2.40	3.318(8)	169
C2–H2···N1A	2.37	3.245(8)	157

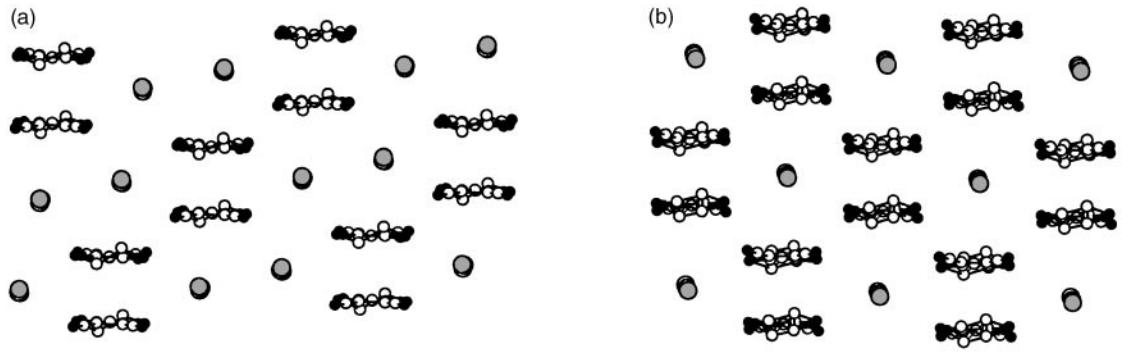

Fig. 2 Views of the 1 : 1 [**1**][I_3] (a) and 2 : 1 [**1**]$_2$[I_3] (b) salts along the long molecular axis of the donor molecules, showing the similar mixed organic–inorganic slabs in both salts with alternating organic diads and I_3^- anions.

organic and anionic inorganic slabs is usually observed,[1] with the formation of conduction bands in the partially oxidised organic slab. In [**1**]$_2$[I_3], the I_3^- anions are interspersed within the organic layers while the mixed-valence diads interact with each other through only two overlap interactions. Calculations of the $\beta_{HOMO\cdots HOMO}$ interaction energies give absolute values of 0.85 eV for the intradimer interaction (interaction I), and 0.32 and 0.23 eV for interactions II and III between dimers (Fig. 5). Those two last values are particularly strong and explain the high conductivity of this salt. However, the large intradimer value most probably tends to localise the spin carrier within each dimer, hence the activated conductivity. Band structure calculations were performed on this system (Fig. 6) and confirm (i) the strong dimerisation with two well separated bands and (ii) the important dispersion of the higher energy band.

The two isostructural salts obtained with $FeBr_4^-$ and $InBr_4^-$ crystallise in the monoclinic system, space group $P2_1/c$ with one donor molecule and one anion in general positions in the unit cell (Fig. 7).[30] The organic radical cations are essentially separated from each other by the tetrahedral anions in the *b*, *c* plane and no specific intermolecular interaction can be identified here, neither CN···Br short contacts

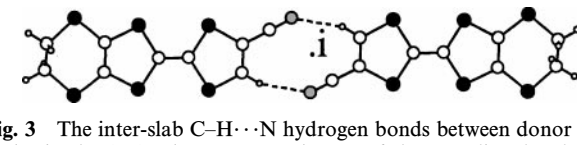

Fig. 3 The inter-slab C–H···N hydrogen bonds between donor molecules in the 1 : 1 salt [**1**][I_3]. Only one of the two disordered rings has been represented for clarity. The inversion centre is represented by .i.

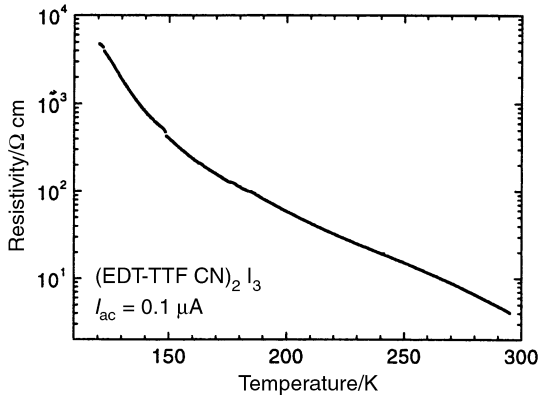

Fig. 4 Temperature dependence of the resistivity of [**1**]$_2$[I_3].

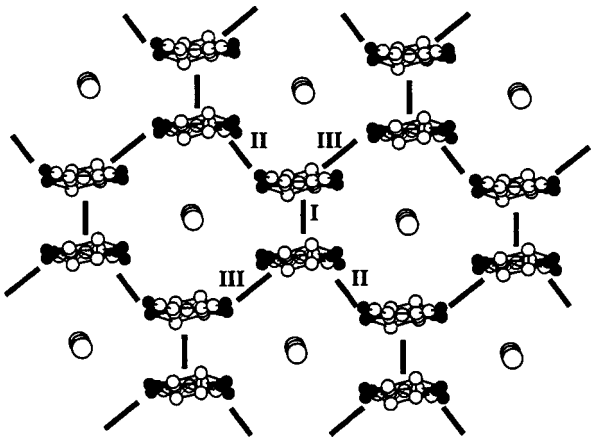

Fig. 5 A view of the hybrid organic–inorganic plane in [**1**]$_2$[I_3] together with the intermolecular interactions I, II and III.

Table 3 Solid state characteristics of the shortest CN···Hal contacts

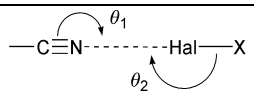

	d(N···Hal)/Å	θ_1/°	θ_2/°
[**1**]$_2$[I_3]	4.27(2), 4.31(2)	81(1), 79(1)	119.4(2), 119.4(2)
[**1**][I_3]	3.96(2)	74(1)	126.1(3)
[**1**][$FeBr_4$]	3.52(1)	81.8(8)	171.9(2)
[**1**][$InBr_4$]	3.445(5)	83.6(4)	172.10(9)
[**1**][$AuBr_4$]	3.728(10)	86.48(2)	109.8(2)
[**1**]$_2$[$Mo_6Cl_8Br_6$][CH_3CN]$_4$	3.56(4), 3.15(4)[a]	137(3), 94(4)[a]	μ_3-Cl atom
[**1**]$_2$[Mo_6Br_{14}][CH_3CN]$_4$	3.43(1), 3.19(1)[a]	142(1), 95(1)[a]	μ_3-Br atom

[a] This contact is between one CH_3CN molecule and μ_3-halide atoms of the $Mo_6Cl_8Br_6^{2-}$ or $Mo_6Br_{14}^{2-}$ anions.

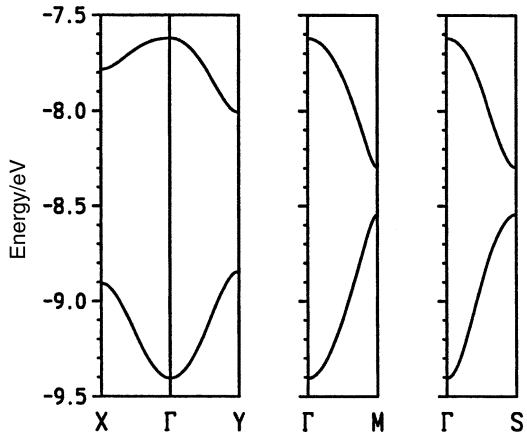

Fig. 6 Calculated band structure for one of the two different donor layers in $[\mathbf{1}]_2[I_3]$. $\Gamma = (0, 0)$, $X = (a^*/2, 0)$, $Y = (0, b^*/2)$, $M = (a^*/2, b^*/2)$ and $S = (-a^*/2, b^*/2)$ where a and b are the repeat vectors of the layer parallel to the direction of interactions III and II, respectively (see Fig. 5). The band structure for the other layer is practically identical.

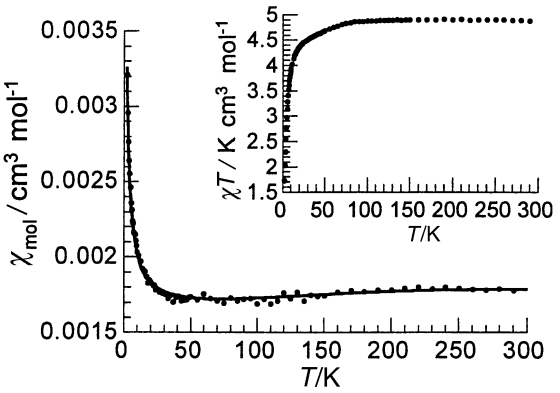

Fig. 8 Temperature dependence of the SQUID magnetic susceptibility of [**1**][$InBr_4$]. The solid line is a fit to the one-dimensional Heisenberg chain together with a Curie contribution at the lowest temperatures. Insert: Temperature dependence of $\chi_{Fe} \cdot T$ in [**1**][$FeBr_4$].

(Table 3) nor C–H···N, Br hydrogen bonds. On the other hand, the radical cations form uniform chains running parallel to the a direction with a sizeable interaction between molecules despite S···S distances above 3.95 Å. The calculated $\beta_{HOMO\cdots HOMO}$ overlap interaction within the chain amounts indeed to 0.16 eV (0.18 eV in the isostructural $FeBr_4^-$ salt). This analysis is further substantiated by the temperature dependence of the magnetic susceptibility of both salts. [**1**][$InBr_4$] exhibits a weakly temperature dependent paramagnetism, which can be properly fitted with the Bonner–Fisher law for uniform chains with $J/k = -514(12)$ K and a low temperature Curie tail encompassing 1.1% magnetic defects (Fig. 8). In the isostructural [**1**][$FeBr_4$] salt, the contribution of the organic spin chain is hidden behind the strong $S = 5/2$ contribution of the $FeBr_4^-$ anions. By subtracting this spin chain contribution from the total susceptibility, we obtain the χ_{Fe} contribution of the $FeBr_4^-$ anion (Fig. 8, insert) with a $\chi_{Fe}T$ value at high temperatures of 4.9 K cm^{-3} mol^{-1}, in good accord with the expected value (4.64 K cm^{-3} mol^{-1}) for an $S = 5/2$ ion with a g value of 2.06, as determined by EPR on the Et_4N^+ salt. The decrease in $\chi_{Fe}T$ at lower temperatures translates the combined effects of the $FeBr_4^-$ zero-field splitting and the eventual presence of $FeBr_4^-/FeBr_4^-$ antiferromagnetic interactions, as already discussed in other $FeBr_4^-$ salts.[31,32]

The 1 : 1 salt with the square planar $AuBr_4^-$ anion crystallises in the triclinic system, space group $P\bar{1}$, with both donor molecule and $AuBr_4^-$ anion in general positions in the unit cell. The radical cations are organised into a, b layers, alternating in the c direction with the $AuBr_4^-$ anions. Here again, no specific hydrogen bonds or CN···Br interactions are observed; the shortest CN···Br distances amount to 3.7–3.8 Å (Table 3). Within one organic layer, the $S = 1/2$ radical cations form a rectangular two-dimensional lattice, characterised by two intermolecular interactions, interaction I running along a, interaction II running along b (Fig. 9). The associated $\beta_{HOMO\cdots HOMO}$ overlap interactions are almost equal, 0.13 and 0.15 eV, respectively, suggesting the presence of a symmetrical square lattice magnetic system. The temperature dependence of the magnetic susceptibility is shown in Fig. 10. It exhibits a maximum around $T_{\chi max} = 120$ K while a finite value is reached at lower temperatures. This behaviour is in accord with the above mentioned magnetic structure.[33] If we consider

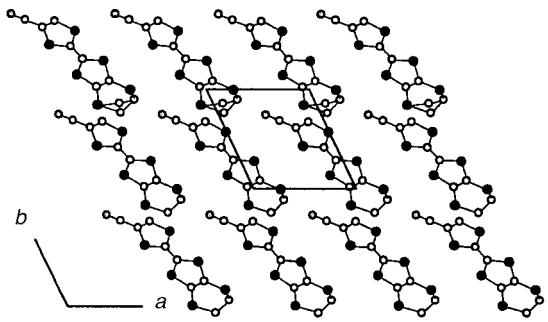

Fig. 9 Projection view (along c) of the unit cell of [**1**][$AuBr_4$] showing the organic plane. The square-planar $AuBr_4^-$ anions have been omitted for clarity.

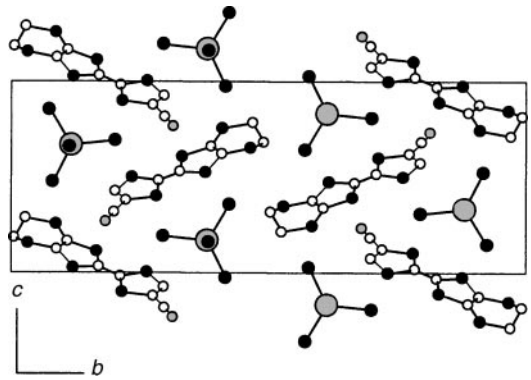

Fig. 7 A projection view of the unit cell of [**1**][$InBr_4$] along the a axis.

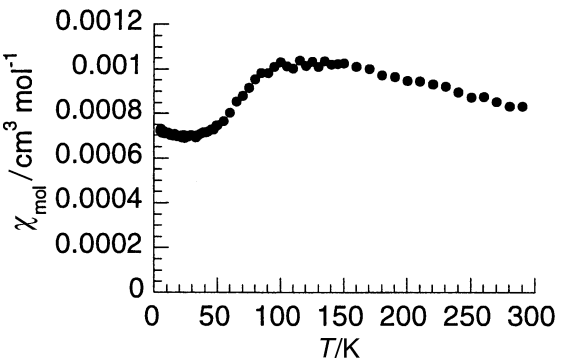

Fig. 10 Temperature dependence of the SQUID magnetic susceptibility of [**1**][$AuBr_4$].

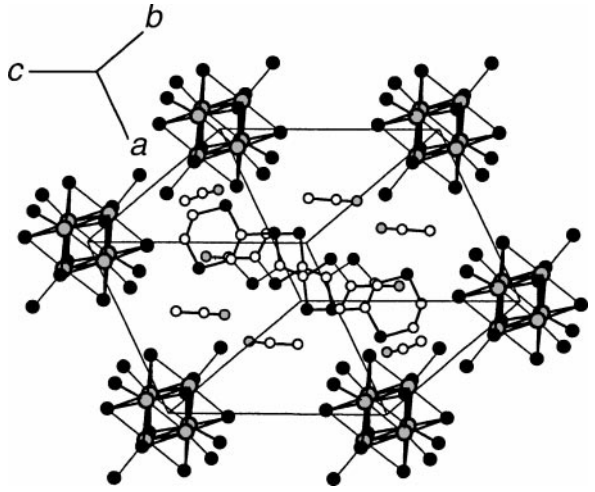

Fig. 11 A view of the unit cell of $[\mathbf{1}]_2[Mo_6Br_{14}][CH_3CN]_4$. Only one of the disordered CH_3CN molecules located in the vicinity of the CN group of **1** has been shown for clarity.

a quadratic Heisenberg layer with antiferromagnetic interactions and $H = \sum_{nn} JS_i \cdot S_j$, then the J value is given by[34] $kT_{\chi max}/J = 1.12\ S(S+1) + 0.10$, affording a J/k value of -127 K.

Finally, **1** forms two isostructural salts with the octahedral cluster anions $Mo_6Cl_8Br_6^{2-}$ and $Mo_6Br_{14}^{2-}$, formulated as $[\mathbf{1}]_2[Mo_6Cl_8Br_6][CH_3CN]_4$ and $[\mathbf{1}]_2[Mo_6Br_{14}][CH_3CN]_4$. They crystallise in the triclinic system, space group $P\bar{1}$ (Fig. 11), with one cation in a general position in the unit cell, one anion cluster located on the inversion centre and two CH_3CN molecules, one located in-between the anion clusters, the other one hydrogen bonded to the hydrogen atom *ortho* to the CN group of $\mathbf{1}^{\cdot+}$. The latter is actually disordered over two positions on the dithiole ring. Here again, the CN group of **1** is not engaged in any CN···Br(Cl) interaction (Table 3), while the shortest N···Br(Cl) contact is actually observed with the CH_3CN molecule included in the anionic layer. The organic radical cations organise in the solid state into inversion-centred diads with a short plane-to-plane distance [3.414(2) and 3.418(2) Å] and a large value of the calculated $\beta_{HOMO\cdots HOMO}$ overlap interaction (0.57 and 0.71 eV) in the $Mo_6Cl_8Br_6^{2-}$ and $Mo_6Br_{14}^{2-}$ salts, respectively, and, as a consequence, a pairing of the two radicals in the bonding combination of the two HOMOs and a diamagnetic behaviour for both salts.

Discussion

As shown in Table 3, in every salt and despite the large number of halogen atoms available, long CN···Hal distances [$\Sigma_{vdW}(N\cdots I) = 3.53$ Å, $\Sigma_{vdW}(N\cdots Br) = 3.40$ Å] and acute CN···Hal angles dismiss the possibility of intermolecular CN···Hal interactions while C–H···N hydrogen bonds are sometimes observed. This absence of CN···Hal interactions is all the more surprising since halogenated TTFs such as EDT-TTF-I or EDO-TTF-I_2 were found to interact[8,9] with cyano anions such as $Au(CN)_2^-$ or $Ni(mnt)_2^{\cdot-}$ with geometrical characteristics typical of the CN···Hal interaction,[13] a N···Hal distance far shorter than the sum of the van der Waals radii together with a strong tendency to linearity ($\theta_1 \approx \theta_2 \approx 180°$). Clearly here, the cyano group in the oxidised $\mathbf{1}^{\cdot+}$ is deactivated for entering into a CN···Hal interaction while this interaction was observed recurrently in the opposite situation with halogenated TTFs. Recent *ab initio* intermolecular perturbation theory calculations[14] showed that the attractive nature of the N···Hal interaction was mainly due to electrostatic effects, while its directionality is explained by the anisotropic electron distribution around the halogen atom, with the lone pair of the nitrogen atom interacting with the positive polarisation of the halogen atom in the polar region. We can therefore understand that the oxidation of **1** to the *cation* radical state can decrease this negative charge density on the nitrogen atom while at the same time, the positive character of the polar zone of the halogen atom is also decreased in the complex *anions*, leading eventually to a suppression of this stabilising interaction. On the other hand, if this is correct, this interaction should be strengthened in the opposite situation involving oxidised halogenated TTF cations with cyanided anions. This is indeed the case. While the N···I distance amounts to 3.18 Å in neutral *p*-iodobenzonitrile,[13] even shorter N···I distances are observed with a *cationic* halide and an *anionic* cyanide, 3.04 Å in [TTF-I]$_2$[Pt(mnt)$_2$],[6] 2.88 Å in [EDT-TTF-I]$_2$[Ag(CN)$_2$] or[8] 3.03 Å in [EDO-TTF-I_2]$_2$[Ni(mnt)$_2$].[9] Similarly, activation of neutral iodinated molecules has also been elegantly achieved by the incorporation of neighbouring strongly electron-withdrawing fluorinated groups, leading also to enhanced N···I interactions.[35,36] All these observations unambiguously confirm the polarised character of the $CN^{\delta-}\cdots{}^{\delta+}$Hal interaction.

DFT calculations were performed on TTF-CN and its radical cation and the results are collected in Table 4, where calculated important bond distances are reported together with the partial charges on the nitrogen atom and the hydrogen atom located *ortho* to the CN group, as deduced from a natural population analysis. We first observe that the bond length distortions of the dithiole ring bearing the CN group, which were observed experimentally in the neutral **1** and the oxidised molecule, are well reproduced as well as the typical C–S bond shortening and central C=C bond lengthening upon oxidation. The stretching frequency increase upon oxidation is also well reproduced, albeit the absolute values are slightly different, a recurrent observation in DFT calculations. Also, as anticipated, the nitrogen atom experiences a notable charge decrease upon TTF oxidation, most probably at the origin of the suppression of the CN···Hal interaction in the salts described here. This behaviour parallels that of other functionalised TTFs such as the amidic EDT-TTF-CONHR for which oxidation to the cation radical was shown to suppress the hydrogen bond acceptor character of the carbonyl function.[5] All these results clearly demonstrate that the efficiency of a given functional group to act in the solid state through an intermolecular interaction can be dramatically modified by changing the oxidation state of the donor molecule, particularly when (i) this group is conjugated with the π-redox TTF core and (ii) the intermolecular interaction possesses an electrostatic contribution, as in hydrogen or halogen bonding. This interdependence between redox state and supramolecular organisation also finds its parallel in biological systems involving redox active enzymes whose actual redox and protonation states strongly depend upon the geometry and balance of weak intermolecular forces, which control the enzyme-cofactor interactions.[37]

Table 4 Geometry optimisation and natural population analysis (DFT calculations) in TTF-CN and [TTF-CN]$^{\cdot+}$ together with the calculated ν(CN). See Fig. 1 for the definition of the a, b, b′, c, c′, d, d′ bonds

	Neutral TTF-CN	[TTF-CN]$^{\cdot+}$
a/Å	1.350	1.398
b, b′/Å	1.789, 1.791	1.746, 1.752
c, c′/Å	1.786, 1.787	1.746, 1.747
d, d′/Å	1.782, 1.740	1.766, 1.731
ν(CN)/cm^{-1}	2290	2306
δ(N)	−0.27	−0.17
δ(H)	+0.28	+0.32

Experimental

Synthesis

All reactions were carried out under nitrogen. Solvents (dichloromethane, acetonitrile) were dried and freshly distilled over P_2O_5. ^1H NMR spectra were recorded at 200 MHz. The chemical shiftsave given in ppm, downfield from internal Me_4Si. Mass spectra were taken in the EI mode with an ionisation energy of 70 eV and a current density of 300 μA. Cyclic voltammetry was carried out with a Pt disk (diam. = 1 mm) as the working electrode, a Pt were as the counter electrode and an SCE as the reference electrode. Elemental analyses were performed at the Institut de Chimie des Substances Naturelles (CNRS), Gif sur Yvette, France.

4-Cyano-2-oxo-1,3-dithiole (3). A solution of **2** (0.5 g, 3.14 mmol) was dissolved in a mixture of $CHCl_3$ (20 mL) and AcOH (7 mL) and treated with $Hg(OAc)_2$ (2.6 g, 8.2 mmol). The solution was stirred overnight, filtered over Celite, washed with H_2O (2 × 50 mL), sat. $NaHCO_3$ (3 × 50 mL) and H_2O (2 × 50 mL), dried over $MgSO_4$. Evaporation to dryness afforded an oil that solidifies upon standing (0.38 g, 85%). M.p. 60–63 °C. ^1H NMR ($CDCl_3$) δ 7.59. MS (EI) *m/z* (int%) 143 (M^+, 100). IR(KBr) ν 2229 (C≡N), 1636 cm^{-1} (C=O). Anal. calc. for C_4HNOS_2 (found): C, 33.57 (33.78); H, 0.70 (0.83); N, 9.79 (9.43); S, 44.76 (43.68)%.

1 and (*Z*,*E*)-(CN)$_2$TTF. A suspension of **4** (0.4 g, 2.8 mmol) and **3** (0.63 g, 2.8 mmol) in freshly distilled $P(OMe)_3$ (8.5 mL) was warmed to 80–85 °C for 6 h. The red suspension was evaporated under vacuum, toluene (40 mL) added and the suspension evaporated again. This operation was repeated twice. Chromatography over SiO_2 (eluent toluene–cyclohexane 2 : 1) afforded first traces of BEDT-TTF, followed by **1** and then (*Z*,*E*)-$(CN)_2$TTF. **1** was recrystallised in toluene (320 mg, 36%) and (*Z*,*E*)-$(CN)_2$TTF in toluene (30 mg, 4%). **1**: M.p. 187 °C. ^1H NMR ($CDCl_3$) δ 7.12 (s, CH, 1H), 3.31 (s, CH_2, 4H). IR(KBr) ν 2214 cm^{-1} (C≡N). Anal. calc. for $C_9H_5NS_6$ (found): C, 33.83 (33.77); H, 1.58 (1.38); N, 4.38 (4.41); S, 60.21 (60.14)%. (*Z*,*E*)-$(CN)_2$TTF: M.p. 230 °C (decomp.). ^1H NMR (d_6-DMSO) δ 8.15 (s, 1H). IR(KBr) ν 2226 cm^{-1} (C≡N). Anal. calc. for $C_8H_2N_2S_4$ (found) C, 37.77 (37.83); H, 0.79 (0.56); N, 11.01 (10.91); S, 50.42 (50.24)%.

Electrocrystallisation experiments. Two-compartment cells with Pt electrodes (l = 2 cm, d = 1 mm) were used. The different electrolytes [Et_4NFeBr_4,[38] Et_4NInBr_4,[39] *n*-Bu_4N-$AuBr_4$,[40] (*n*-$Bu_4N)_2(Mo_6Cl_8Br_6)$ and[41] (*n*-$Bu_4N)_2$-(Mo_6Br_{14})][42] were prepared according to published procedures and recrystallised twice before use. Solvents were dried over activated Al_2O_3 and degassed. Specific conditions are collected in Table S1 in the ESI.

X-Ray crystallography

Details of data collection and structure refinement are given in Table 5. Data were collected on a Stoe-IPDS or an Enraf–Nonius Mach 3 diffractometer at 293 K with graphite-monochromated Mo-Kα radiation (λ = 0.710 73 Å). The Stoe software was used for data collection and reduction, and numerical absorption correction using crystal faces was applied to all structures except for [**1**][$FeBr_4$] and [**1**]$_2$[$Mo_6Cl_8Br_6$]. For the latter, using an Enraf–Nonius Mach 3 diffractometer, reduction of the data was performed with XCAD4[43] and absorption correction from a ψ scan applied (SHELXPREP).[44] The structure was solved using direct methods (SHELXS)[45] and refined using SHELXL.[46] All atoms except hydrogen atoms were refined anisotropically. Hydrogen atoms were introduced at calculated positions (riding model) and not refined. In both salts with I_3^-, the CN group is disordered over the two possible carbon positions, with a 60 : 40 and 50 : 50 distribution in the 1 : 1 and 2 : 1 salts, respectively. The ethylene bridge of both donor molecules is disordered in both I_3^- and was refined isotropically. Similarly, in [**1**][$AuBr_4$], one of the carbon atoms of the ethylenic bridge is disordered over two position with a 50 : 50 occupation parameter.

CCDC reference numbers 170662–170669. See http://www.rsc.org/suppdata/nj/b1/b104640n/ for crystallographic data in CIF or other electronic format.

Magnetic susceptibility measurements

Magnetic susceptibility measurements were performed on a Quantum Design MPMS5 SQUID magnetometer operating in the range 5–300 K with polycrystalline samples. Data were corrected for Pascal diamagnetism and sample holder contribution.

Theoretical calculations

The overlap interaction energies ($\beta_{\text{HOMO-HOMO}}$) and tight-binding band structure calculations[47] were of the extended-Hückel type.[48] A modified Wollsberg–Helmholtz formula was used to calculate the non-diagonal $H_{\mu\nu}$ values.[49] Double-ζ orbitals for C, S and N were used. DFT calculations were performed with GAUSSIAN98[50] using the 6-31G* basis and the B3LYP functional with a Becke gradient correction for exchange[51] and Lee–Yang–Parr corrections for correlation.[52]

Table 5 Crystallographic data for neutral **1** and its salts

	1	[**1**]$_2$[I_3]	[**1**][I_3]	[**1**][$InBr_4$]	[**1**][$FeBr_4$]	[**1**][$AuBr_4$]	[**1**]$_2$[Mo_6Br_{14}] [CH_3CN]$_4$	[**1**]$_2$[$Mo_6Cl_8Br_6$] [CH_3CN]$_4$
Formula	$C_9H_5NS_6$	$C_{18}H_{10}I_3N_2S_{12}$	$C_9H_5I_3NS_6$	$C_9H_5Br_4InNS_6$	$C_9H_5Br_4FeNS_6$	$C_9H_5AuBr_4Ns_6$	$C_{13}H_{11}Br_7Mo_3N_3S_6$	$C_{13}H_{11}Br_3Cl_4Mo_3N_3S_6$
Formula mass	319.50	1019.7	700.20	753.96	694.99	836.11	1248.8	1070.96
Crystal system	Triclinic	Triclinic	Triclinic	Monoclinic	Monoclinic	Triclinic	Triclinic	Triclinic
Space group	$P\bar{1}$	$P\bar{1}$	$P\bar{1}$	$P2_1/c$	$P2_1/c$	$P\bar{1}$	$P\bar{1}$	$P\bar{1}$
a/Å	6.9395(14)	8.0545(16)	7.9359(16)	6.3990(13)	6.2930(13)	7.7596(16)	10.191(2)	9.9799(10)
b/Å	7.6083(15)	8.0611(16)	9.4229(19)	28.687(6)	28.506(6)	8.3250(17)	11.443(2)	11.3713(10)
c/Å	12.502(3)	23.587(5)	11.957(2)	11.222(2)	11.126(2)	16.245(3)	13.372(3)	13.3427(10)
α/°	104.45(3)	86.78(3)	99.04(3)	—	—	93.98(3)	102.05(3)	101.938(10)
β/°	93.03(3)	86.82(3)	94.56(3)	106.13(3)	106.52(3)	93.63(3)	103.82(3)	104.094(10)
γ/°	95.46(3)	76.11(3)	103.70(3)	—	—	114.98(3)	93.63(3)	93.366(10)
U/Å^3	634.3(2)	1482.9(5)	851.5(3)	1978.9(7)	1913.5(7)	944.0(3)	1470.2(5)	1427.3(2)
Z	2	2	2	4	4	2	2	2
μ/mm^{-1}	1.046	4.023	6.226	9.894	9.785	16.911	11.21	6.322
Reflect. collected	5854	12 816	8345	15 693	3859	9269	17 757	6520
Indep. reflect.	2170	5233	3083	3702	3757	3409	6538	5531
R_{int}	0.0582	0.0459	0.0516	0.0482	0.1134	0.099	0.0434	0.0506
Obs. reflect. [$I > 2\sigma(I)$]	1501	2659	1998	2399	2124	2363	3838	2926
$R(F)$	0.0559	0.0359	0.0254	0.0276	0.0486	0.0445	0.0273	0.0622
$wR(F^2)$	0.134	0.1326	0.0505	0.0611	0.1043	0.1139	0.0511	0.2044

Initial geometries were obtained through a molecular mechanics minimisation (AM1, Chem3DUltra). A UHF optimisation was also performed on $[TTF\text{-}CN]^{\cdot+}$ before DFT calculations. A vibrational analysis was done at the same level. Calculated values were scaled by 0.98. Reed and Weinhold's NBO analysis was performed.[53]

Acknowledgements

We thank the CNRS and the Région Pays de Loire for financial support. This work was supported (E. C.) by DGI-Spain (Project BFM2000-1312-C02-01) and Generalitat de Catalunya (Project 1999 SGR 207). Financial support (to T. D.) by the Ecole Normale Supérieure de Lyon (France) is gratefully acknowledged.

References and notes

1 J. M. Williams, J. R. Ferraro, R. J. Thorn, K. D. Carlson, U. Geiser, H. H. Wang, A. M. Kini and M.-H. Whangbo, in *Organic Superconductors* (*Including Fullerenes*), Prentice Hall, Engelwood Cliffs, NJ, 1992; *Supramolecular Engineering of Synthetic Metallic Materials*, ed. J. Veciana, C. Rovira and D. B. Amaloilino, NATO ASI Ser., vol. 518, Kluwer, Dordrecht, 1999.
2 M. R. Bryce, *J. Mater. Chem.*, 1995, **5**, 1481.
3 P. Blanchard, K. Boubekeur, M. Sallé, G. Duguay, M. Jubault, A. Gorgues, J. D. Martin, E. Canadell, P. Auban-Senzier, D. Jérome and P. Batail, *Adv. Mater.*, 1992, **4**, 579.
4 A. Dolbecq, A. Guirauden, M. Fourmigué, K. Boubekeur, P. Batail, M.-M. Rohmer, M. Bénard, C. Coulon, M. Sallé and P. Blanchard, *J. Chem. Soc., Dalton Trans.*, 1999, 1241.
5 K. Heuzé, C. Mézière, M. Fourmigué, P. Batail, C. Coulon, E. Canadell, P. Auban-Senzier and D. Jérome, *Chem. Mater.*, 2000, **12**, 1898; K. Heuzé, M. Fourmigué, P. Batail, E. Canadell and P. Auban-Senzier, *Chem. Eur. J.*, 2000, **5**, 2971.
6 A. J. Moore, M. R. Bryce, A. S. Batsanov, J. N. Heaton, C. W. Lehman, J. A. K. Howard, N. Roberston, A. E. Underhill and I. F. Perepichka, *J. Mater. Chem.*, 1998, **8**, 1541.
7 A. S. Batsanov, A. J. Moore, N. Roberston, A. Green, M. R. Bryce, J. A. K. Howard and A. E. Underhill, *J. Mater. Chem.*, 1997, **7**, 387.
8 T. Imakubo, H. Sawa and R. Kato, *J. Chem. Soc., Chem. Commun.*, 1995, 1097; T. Imakubo, H. Sawa and R. Kato, *Synth. Met.*, 1997, **86**, 1847.
9 Y. Kuwatani, E. Ogura, H. Nishikawa, I. Ikemoto and M. Iyoda, *Chem. Lett.*, 1997, 817; J. Nishijo, E. Ogura, J. Yamaura, A. Miyazaki, T. Enoki, T. Takano, Y. Kuwatani and M. Iyoda, *Solid State Commun.*, 2000, **116**, 661.
10 T. Imakubo, H. Sawa and R. Kato, *J. Chem. Soc., Chem. Commun.*, 1995, 1667.
11 S. L. Price, A. J. Stone, J. Lucas, R. S. Rowland and A. E. Thornley, *J. Am. Chem. Soc.*, 1994, **116**, 4910; G. R. Desiraju and R. Parthasarathy, *J. Am. Chem. Soc.*, 1989, **111**, 8725.
12 B. Domercq, T. Devic, M. Fourmigué, P. Auban-Senzier and E. Canadell, *J. Mater. Chem.*, 2001, **11**, 1570.
13 G. R. Desiraju and R. L. Harlow, *J. Am. Chem. Soc.*, 1989, **111**, 6757.
14 J. P. M. Lommerse, A. J. Stone, R. Taylor and F. H. Allen, *J. Am. Chem. Soc.*, 1996, **118**, 3108.
15 G. R. Desiraju and T. Steiner, *The Weak Hydrogen Bond*, Oxford Science Publ., Oxford, 1999.
16 O. Hassel, *Mol. Phys.*, 1958, **1**, 241; O. Hassel and C. Romming, *Rev. Chem. Soc.*, 1962, **16**, 1.
17 D. Britton, *Perspect. Struct. Chem.*, 1967, **1**, 109.
18 G. Cooke, A. K. Powell and S. L. Heath, *Synthesis*, 1995, 1411.
19 Z. J. Zhong, X.-Z. You and K. Yu, *Acta Crystallogr., Sect. C*, 1996, **52**, 449.
20 See also: N. Terkia-Derdra, R. Andreu, M. Sallé, E. Levillain, J. Orduna, J. Garin, E. Orti, R. Viruela, R. Pou-Amerigo, B. Sahraoui, A. Gorgues, J.-F. Favard and A. Riou, *Chem. Eur. J.*, 2000, **6**, 1199.
21 B. A. Scott, F. B. Kaufman and E. M. Engler, *J. Am. Chem. Soc.*, 1976, **98**, 4342; S. Yoneda, T. Kawase, M. Inaba and Z. Yoshida, *J. Org. Chem.*, 1978, **43**, 595.
22 M. Fourmigué and J. N. Bertran, *Chem. Commun.*, 2000, 2111.
23 The folding angles of the two dithiole rings along the S···S hinge amount to $\alpha = 2.5(2)^\circ$ for the dithiole ring bearing the CN group, $\beta = 5.24(8)^\circ$ for the other one.
24 A. S. Batsanov, M. R. Bryce, J. N. Heaton, A. J. Moore, P. J. Skabara, J. A. K. Howard, E. Orti, P. M. Viruela and R. J. Viruela, *J. Mater. Chem.*, 1995, **5**, 1689.
25 K. Heuzé, M. Fourmigué and P. Batail, *J. Mater. Chem.*, 1999, **9**, 2373.
26 G. Le Costumer and Y. Mollier, *J. Chem. Soc., Chem. Commun.*, 1980, 38.
27 The possible transformation of the triclinic unit cell into a C-centred monoclinic one with only one donor molecule in a general position and one I_3^- anion on an inversion centre did not afford satisfactory refinements.
28 H. Guth, G. Heger and U. Drück, *Z. Kristallogr.*, 1982, **159**, 185.
29 M.-H. Whangbo, J. M. Williams, P. C. W. Leung, M. A. Beno, T. J. Emge and H. H. Wang, *Inorg. Chem.*, 1985, **24**, 3500.
30 Note that the actual conventional description for the $FeBr_4^-$ salt is actually $P2_1/n$ with a unit cell very close to that observed in the $P2_1/c$ description: $a = 6.2928(10)$, $b = 28.5061(10)$, $c = 11.1155(10)$ Å, $\beta = 106.348(10)^\circ$.
31 C. Mézière, M. Fourmigué, E. Canadell, R. Clérac, K. Bechgaard and P. Auban-Senzier, *Chem. Mater.*, 2000, **12**, 2250.
32 J. J. Borras Almenar, J. M. Clemente-Juan, E. Coronado and B. D. Tsukerblat, *Inorg. Chem.*, 1999, **38**, 6081.
33 L. J. De Jongh and A. R. Miedema, *Adv. Phys.*, 1974, **23**, 1.
34 M. E. Lines, *J. Phys. Chem. Solids*, 1970, **31**, 101.
35 E. Corradi, S. V. Meille, M. T. Messina, P. Metrangolo and G. Resnati, *Angew. Chem., Int. Ed.*, 2000, **39**, 1783.
36 R. B. Walsh, C. W. Padgett, P. Metrangolo, G. Resnati, T. W. Hanks and W. T. Pennington, *Cryst. Growth Des.*, 2001, **1**, 165.
37 A. Niemz and V. M. Rotello, *Acc. Chem. Res.*, 1999, **32**, 44.
38 T. Mallah, C. Hollis, S. Bott, M. Kurmoo, P. Day, M. Allan and R. H. Friend, *J. Chem. Soc., Dalton Trans.*, 1990, 859.
39 J. Gislason, M. H. Lloyd and D. G. Tuck, *Inorg. Chem.*, 1971, **10**, 1907.
40 P. Braunstein and R. J. H. Clark, *J. Chem. Soc., Dalton Trans.*, 1973, 1845.
41 F. A. Cotton, R. M. Wing and R. A. Zimmerman, *Inorg. Chem.*, 1967, **6**, 11.
42 J. C. Sheldon, *J. Chem. Soc.*, 1962, 410.
43 K. Harms, XCAD4, Program for Data Reduction, University of Marburg, Germany, 1993.
44 SHELXPREP, Program for Data Preparation and Reciprocal Space Exploration, ver. 5.10, Bruker Analytical X-ray Systems, Madison, WI, 1997.
45 G. M. Sheldrick, SHELXS97, Program for Crystal Structure Resolution, University of Göttingen, Germany, 1986–1997.
46 G. M. Sheldrick, SHELXL97, Program for Crystal Structure Refinement, release 97-2, University of Göttingen, Germany, 1993–1997.
47 M.-H. Whangbo and R. Hoffmann, *J. Am. Chem. Soc.*, 1978, **100**, 6093.
48 R. Hoffmann, *J. Chem. Phys.*, 1963, **39**, 1397.
49 J. H. Ammeter, H.-B. Bürgi, J. Thibeault and R. Hoffmann, *J. Am. Chem. Soc.*, 1978, **100**, 3686.
50 M. J. Frisch, G. W. Trucks, H. B. Schlegel, G. E. Scuseria, M. A. Robb, J. R. Cheeseman, V. G. Zakrzewski, J. A. Montgomery, Jr., R. E. Stratmann, J. C. Burant, S. Dapprich, J. M. Millam, A. D. Daniels, K. N. Kudin, M. C. Strain, O. Farkas, J. Tomasi, V. Barone, M. Cossi, R. Cammi, B. Mennucci, C. Pomelli, C. Adamo, S. Clifford, J. Ochterski, G. A. Petersson, P. Y. Ayala, Q. Cui, K. Morokuma, D. K. Malick, A. D. Rabuck, K. Raghavachari, J. B. Foresman, J. Cioslowski, J. V. Ortiz, A. G. Baboul, B. B. Stefanov, G. Liu, A. Liashenko, P. Piskorz, I. Komaromi, R. Gomperts, R. L. Martin, D. J. Fox, T. Keith, M. A. Al-Laham, C. Y. Peng, A. Nanayakkara, C. Gonzalez, M. Challacombe, P. M. W. Gill, B. Johnson, W. Chen, M. W. Wong, J. L. Andres, C. Gonzalez, M. Head-Gordon, E. S. Replogle and J. A. Pople, GAUSSIAN 98, Rev. A.7, Gaussian, Inc., Pittsburgh PA, 1998.
51 A. D. Becke, *Phys. Rev. B*, 1986, **33**, 8822; A. D. Becke, *ACS Sym. Ser.*, 1989, **394**, 165; A. D. Becke, *Int. J. Quantum Chem.*, 1989, Symp. no. 23, 599.
52 C. Lee, W. Yang and R. G. Parr, *Phys. Rev. B*, 1988, **41**, 785.
53 A. E. Reed, R. B. Weinstock and F. Weinhold, *J. Chem. Phys.*, 1985, **83**, 735; A. E. Reed and F. Weinhold, *J. Chem. Phys.*, 1985, **83**, 1736; A. E. Reed, L. A. Curtis and F. Weinhold, *Chem. Rev.*, 1988, **88**, 899.